Current Biology 17, 462–467, March 6, 2007 ©2007 Elsevier Ltd All rights reserved DOI 10.1016/j.cub.2007.01.069

Report

Modulation of Lateral Diffusion in the Plasma Membrane by Protein Density

Manfred Frick,[1] Katja Schmidt,[1,2] and Benjamin J. Nichols[1,*]

[1] Medical Research Council Laboratory of Molecular Biology
Hills Road
Cambridge CB2 2QH
United Kingdom

Summary

The rate of lateral diffusion of proteins over micron-scale distances in the plasma membrane (PM) of mammalian cells is much slower than in artificial membranes [1, 2]. Different models have been advanced to account for this discrepancy. They invoke either effects on the apparent viscosity of cell membranes through, for example, protein crowding [3, 4], or a role for cortical factors such as actin or spectrin filaments [1]. Here, we use photobleaching to test specific predictions of these models [5]. Neither loss of detectable cortical actin nor knockdown of spectrin expression has any effect on diffusion. Disruption of the PM by formation of ventral membrane sheets or permeabilization induces aggregation of membrane proteins, with a concomitant increase in rates of diffusion for the nonaggregated fraction. In addition, procedures that directly increase or decrease the total protein content of the PM in live cells cause reciprocal changes in lateral diffusion rates. Our data imply that slow diffusion over micron-scale distances is an intrinsic property of the membrane itself and that the density of proteins within the membrane is a significant parameter in determining rates of lateral diffusion.

Results and Discussion

FRAP as an Assay for Lateral Diffusion

FRAP, fluorescence recovery after photobleaching, can be used for measuring the average rates of lateral diffusion for populations of molecules within the plasma membrane (PM) [1, 5]. Various analytical approaches to FRAP data have been developed to take into account factors such as non-Brownian diffusion and the apparent slowly diffusing or "immobile" fraction [6], topology of the photobleached region [7], and recovery during the time taken for photobleaching [8]. In our experiments, diffusion was assayed with FRAP of circular regions of approximately flat plasma membrane, and recovery curves could be fitted to a single exponential (Figure S1 in the Supplemental Data available online) [5, 9–11]. The immobile fraction was in the range of 10%–20% for all of the proteins studied and did not vary significantly in any of our experiments. It is not clear whether this small "immobile" fraction represents a population of slowly diffusing molecules in the membrane, the presence of the PM proteins in small intracellular vesicles within the bleach region, or a combination of these factors [6, 10]. The diffusion coefficient D, derived from fitting to a single exponential, provides a good measure of the average rates of diffusion over micron-scale distances [5, 11, 12] and may reflect a combination of different diffusive phenomena detectable over smaller time and distance scales [1, 2, 6]. Our values for D are consistent with those obtained in other recent FRAP studies, as well as non-FRAP measurements of micron-scale diffusion in cells [10, 12–14]. These rates of diffusion are faster than those determined in several early FRAP experiments [5, 15], but they are still approximately an order-of-magnitude slower than those obtained when, for example, GPI-linked proteins are reconstituted into liposomes [16].

Cortical Cytoskeleton Has No Effect on Lateral Diffusion Assayed by FRAP

We expressed four GFP fusion proteins, each with a different membrane topology (Figure 1A) in COS-7 cells. Disruption of the actin cytoskeleton with latrunculin A or stabilization of actin bundles with jasplakinolide had no detectable effect on D (Figure 1B) [9, 17, 18]. Total internal reflection (TIR) imaging showed that 1 μM latrunculin is sufficient for removal of greater than 90% of phalloidin-stainable actin filaments within the plane of TIR illumination (Figure S2A). It has been proposed that cortical actin does have an effect on lateral diffusion [1, 19] so we sought additional approaches. Depletion of the protein septin2 with siRNAs causes profound changes in the distribution of cortical actin and reduces actin expression levels to less than half of those found in control cells [20, 21]. These effects were also seen in the COS-7 cells used here (data not shown). Despite this, there was no change in D for any of the constructs tested in these cells (Figure 1C). Additionally, cells were microinjected with an N-terminal fragment of gelsolin [22]. This caused a loss of more than 95% of phalloidin-stainable actin filaments (Figure 1D) and caused rapid changes in cell morphology [22]. FRAP on microinjected cells expressing the LYFPGT46 chimaera showed that even this massive disruption of the actin cytoskeleton has no effect on average rates of lateral diffusion (Figure 1E).

The data presented above argue against a role for cortical actin in limiting lateral diffusion over micron-scale distances and raise the possibility that such diffusion is in fact not determined by the cortical cytoskeleton. To investigate this further, we used a cell line, M2, that lacks the actin-binding protein filamin. Filamin is essential for formation of an orthogonal network of actin fibers in the cell cortex, and M2 cells produce large, dynamic membrane blebs that correspond to regions where interaction between the PM and the cortex is absent or perturbed (Figure 1F) [23]. FRAP within thin confocal

*Correspondence: ben@mrc-lmb.cam.ac.uk
[2] Current address: Novartis Pharma GmbH, BU Oncology, Roonstr. 25, 90429 Nuernberg, Germany.

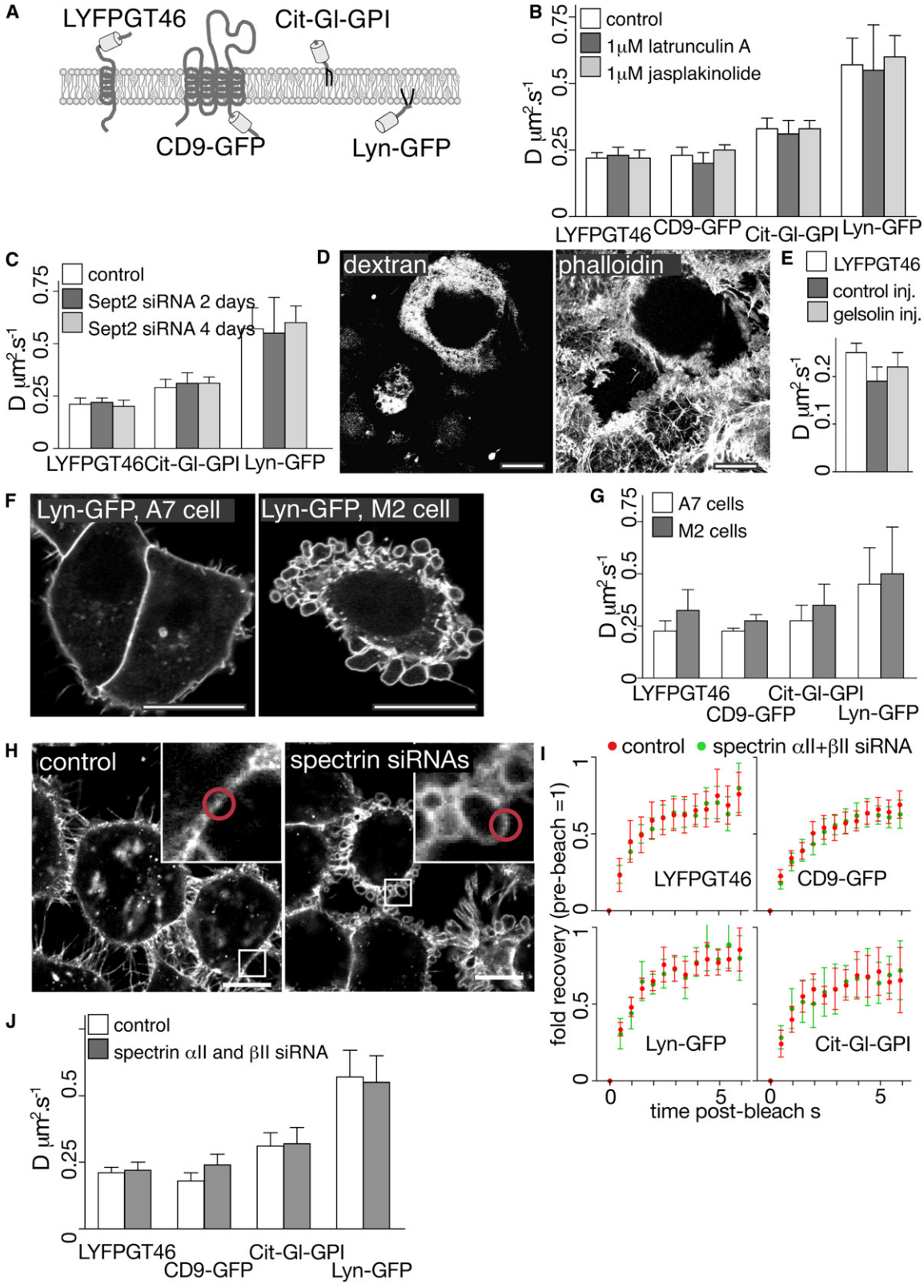

Figure 1. Cortical Cytoskeleton Has No Effect on Lateral Diffusion Measured by FRAP

(A) Chimaeric proteins used in this study. LYFPGT46 (based on the transmembrane domain of the LDL receptor) and YFP-Gl-GPI are described by Keller et al. [31]. CD9-GFP is from I. Tachibana, and Lyn-GFP, which contains the entire Lyn protein, is from T. Meyer.

(B) Effect of actin depolymerization with latrunculin A (1 μm) or actin-filament stabilization with Jasplakinolide (1 μm) on diffusion coefficient D for chimaeric proteins. Error bars represent SD; n > 10. We used several different latrunculin concentrations (0.1–2 μM) and incubation times with the same result.

sections of M2 cell blebs and within the PM of control A7 cells (M2 cells stably transfected with filamin [23]; see Figure S2B) showed that lateral diffusion was not significantly different between M2 cell blebs and A7 cells (Figure 1G).

Spectrin polymers slow diffusion of membrane components in erythrocytes [24, 25]. In order to investigate whether this is the case in other cells, we used siRNAs against the predominant nonerythroid spectrin isoforms, αII and βII (Figure S3). Efficient knockdown of spectrin expression induced large and highly dynamic membrane blebs in approximately 35% of the cells, presumably as a consequence of failure of the cortical cytoskeleton to maintain membrane and cell shape (Figure 1H; see also Movie S1). We measured lateral diffusion both at the flat base of the siRNA-transfected cells and within membrane blebs. The blebs were constantly moving (Movie S1), hindering accurate measurement of complete recovery in FRAP experiments, but both D at the base of the cells and initial rates of recovery after photobleaching within blebs were the same in control and siRNA-treated cells in the case of three of the four proteins studied, with the CD9 construct showing a slight but reproducible increase in D (Figures 1I and 1J). Thus spectrins, like actin, do not have a major effect on average rates of lateral diffusion of diverse membrane components over micron-scale distances in nonerythroid cells.

The results outlined above, obtained from blebs induced by absence or reduction in expression of specific cortical proteins, are in contrast to a previous study where diffusion in blebs induced by low concentrations of formaledehyde and divalent metal ions was found to be significantly quicker than diffusion in the adjacent cell body [15]. We found, however, that blebs induced by this latter method exhibited a striking reduction in protein-to-lipid ratio (Figure S4A) and that the formaldehyde treatment was itself sufficient to slow diffusion in the cell body (Figure S4B). Thus, although we could reproduce the previously reported changes in diffusion of ConA in chemically induced blebs [15], these effects may be explained by factors other than the absence of cytoskeleton in the blebs, including changes in protein surface density.

Reduction in Protein Density Correlates with Faster Diffusion in Semi-Intact Cell Systems

The data presented above suggest that the average rates of diffusion derived from FRAP experiments are a result of the intrinsic properties of the membrane, rather than interaction with the cell cortex. This hypothesis was tested with two different semi-intact cell systems: Either cells were permeabilized with streptolysin O, or ventral membrane sheets were prepared using washes with hypotonic medium [26]. There was a marked increase in D for all of the constructs assayed in both permeabilized cells and membrane sheets (Figures 2A and 2B). In contrast, addition of energy poisons did not alter D (Figure 2A). Actin and spectrin distribution was not visibly perturbed in either semi-intact cell system (Figures S5A and S5B). Addition of gelsolin [27], which removed over 95% of phalloidin or antibody-stainable actin and over 80% of both αII and βII spectrins (Figures S5A and S5B), but did not further alter D (Figures 2A and 2B). These surprising results do not reveal which factors cause the increase in D, but such factors are unlikely to include perturbation of the cortical cytoskeleton because near-complete removal of actin and spectrins from membrane sheets had no further effect on diffusion.

The increases in lateral diffusion observed for all chimaeric proteins studied in semi-intact cell systems provide direct confirmation of the premise that one or more factors slow diffusion in intact cells and also provide an opportunity for identifying these factors [1, 2, 28]. The most obvious change in the distribution of all of the GFP chimaeras in both types of semi-intact cell system was the appearance of bright puncta, apparently in the plane of the PM (Figure 2C). Bright puncta were excluded from the photobleached area. Use of amine-reactive fluorophore to nonspecifically label all cell-surface proteins revealed the same phenomenon for endogenous PM proteins (Figure 2D). Both comparison of membrane lipid and protein distribution with DiI- and GFP-tagged membrane proteins, and measurements of FRET as an assay for clustering of proteins [29], showed that many of the bright puncta represent regions of the membrane with sharply increased protein-to-lipid ratio and protein density (Figures S6A and S6B). This suggests that they represent nonspecific aggregation of proteins in the PM. The appearance of protein aggregates and concomitant increases in lateral diffusion can be explained if protein density within the membrane plays a role in limiting lateral diffusion because partial aggregation would cause a reduction in total membrane protein density in those regions of the membrane not containing aggregates (the areas where FRAP was performed) and hence an increase in the rate of diffusion.

(C) Effect of septin 2 siRNAs on diffusion coefficient D for chimaeric proteins. FRAP was carried out at both 2 and 4 days after transfection with siRNAs. Error bars represent SD; n > 10.

(D) Microinjection of the N-terminal portion of gelsolin destroys the actin cytoskeleton. Dextran shows microinjected cells, cells stained with phalloidin to visualize filamentous actin. A thin confocal section of the base of the cells is shown. Scale bars represent 20 μm.

(E) Effect of destruction of the actin cytoskeleton by gelsolin N-terminal domain microinjection on diffusion coefficient D for LYFPGT46 protein. Error bars represent SD; n > 6.

(F) PM morphology in A7 and M2 cells. M2 cells lack the actin-binding protein filamin. Lyn-GFP is used for labeling the PM. Scale bars represent 20 μm.

(G) Comparison of rates of lateral diffusion (D) between M2 cell blebs and A7 cells, for four different proteins. n = 10; error bars represent SD.

(H) Surface labeling of control cells and cells transfected with spectrin αII and βII siRNA. PM was labeled with CD59 antibodies to allow visualization of the large blebs induced by the spectrin siRNAs. Inserted panels show regions of the PM used in typical photobleaching experiments (see also Figure S2B). Scale bars represent 20 μm.

(I) Initial rates of recovery of four different GFP fusion proteins in control cells and spectrin-siRNA-induced blebs (with FRAP of thin confocal sections as illustrated in the case of M2 cell blebs in Figure 1I). Mean and 95% confidence intervals are shown for each data point; n = 10.

(J) Comparison of rates of lateral diffusion (D) between cells transfected with the control and spectrin αII + βII siRNAs. FRAP was carried out at the flat base of both cell populations rather than in membrane blebs. n = 15; error bars represent SD.

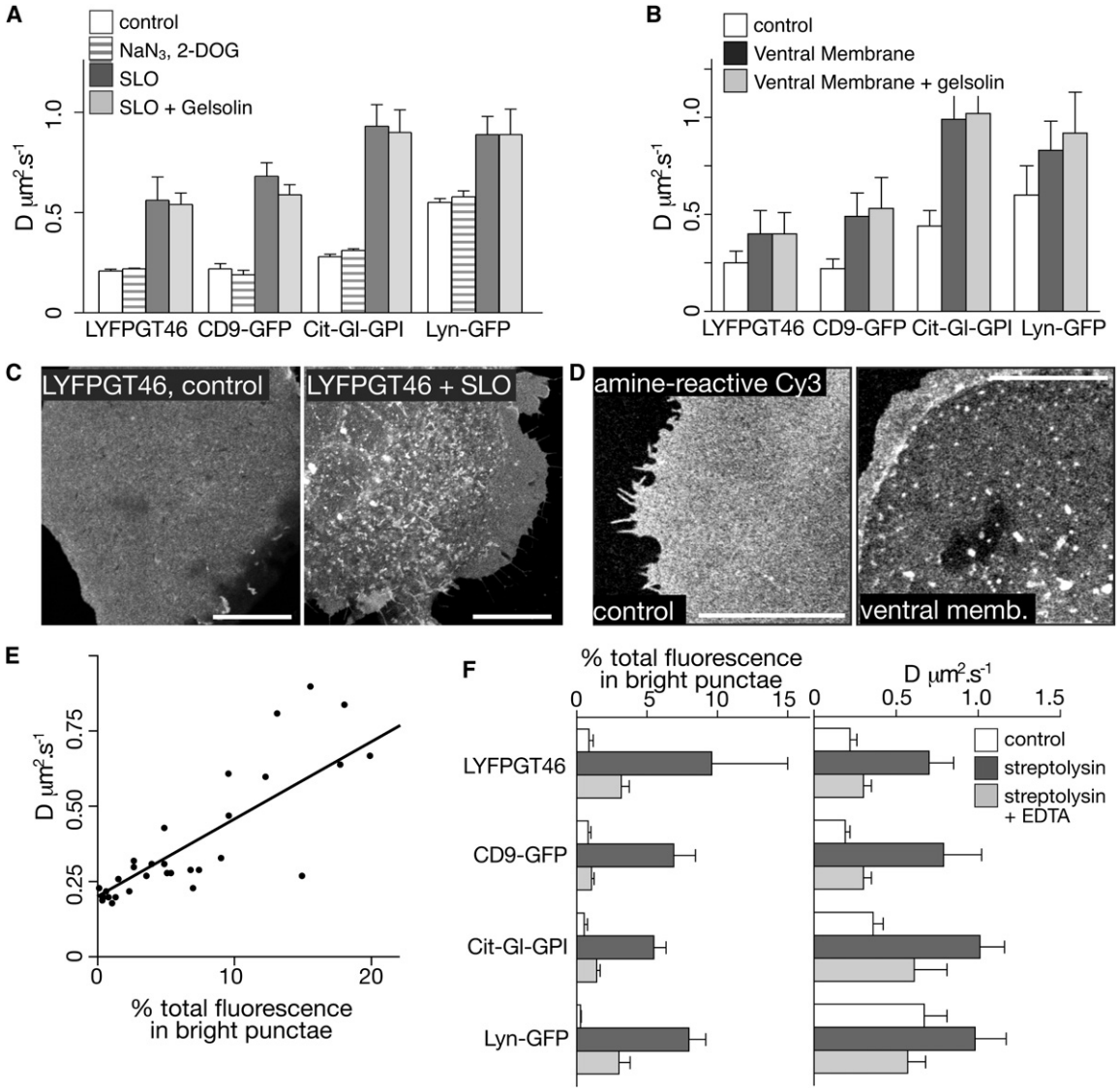

Figure 2. Disruption of the PM Increases Lateral Diffusion Independently from the Actin Cytoskeleton

(A) Effect of cell permeabilization with streptolysin O (SLO), energy poisons, and the removal of actin with gelsolin on diffusion coefficient D for chimaeric proteins. Error bars represent SD; n > 10.

(B) Effect of isolation of ventral PM sheets and subsequent removal of actin with gelsolin on diffusion coefficient D for chimaeric proteins. Error bars represent SD; n > 10.

(C) Effect of permeabilization with streptolysin O (SLO) on distribution of LYFPGT46 protein. Similar bright puncta were seen with other chimaeric proteins and when ventral PM sheets were isolated. Live, unfixed cells are shown. Scale bars represent 10 μm.

(D) Aggregation of endogenous PM proteins in ventral membrane sheets. The cell surface was labeled with amine-reactive Cy3 to allow nonspecific detection of proteins. Similar aggregation was also seen in streptolysin-O-permeabilized cells. Scale bars represent 10 μm. A live cell (control) and unfixed membrane sheet are shown.

(E) Correlation between aggregation of chimaeric proteins into bright puncta induced by cell disruption and lateral mobility of the nonaggregated fraction (D). Spearman's correlation coefficient for the data shown is equal to 0.86, $p < 0.0001$.

(F) Correlation between changes in the aggregation of chimaeric proteins induced by cell permeabilization with streptolysin O in the presence and absence of EDTA (left panel) and lateral mobility of the nonaggregated fraction (right panel). Error bars represent SD; n > 10.

Indeed, plotting D against the percentage of protein in aggregates revealed that there is a direct correlation between these parameters (Figure 2E).

Initial characterization of the factors responsible for protein aggregation in semi-intact cells showed that divalent metal ions may be involved because disruption of the membrane in the presence of EDTA partially blocked the formation of aggregates (Figure 2F). Although the cause of nonspecific protein aggregation is unclear, the effect of EDTA allowed us to again confirm the direct correlation between aggregation and increases in rates of diffusion for the nonaggregated fraction (Figure 2F). This is fully consistent with the model outlined above, a model in which partial aggregation of proteins in the membrane reduces protein density outside the aggregates and thereby increases rates of lateral diffusion.

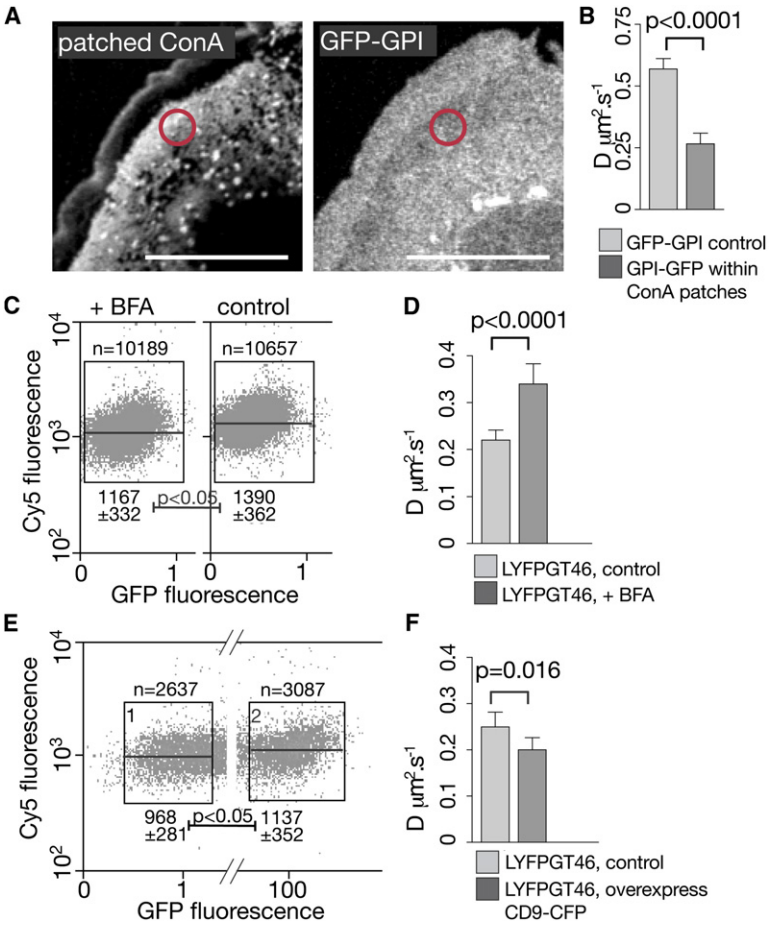

Figure 3. Surface Density of Membrane Proteins Modulates Lateral Diffusion Measured by FRAP

(A) Patching of ConA receptors with biotinylated ConA and Cy5-conjugated streptolysin does not lead to patching of GPI-linked GFP. Typical regions used for photobleaching experiments for determining D in the patched regions are shown as red circles. Scale bars represent 20 μm.

(B) Increase in density of ConA receptors in patches is sufficient to greatly slow diffusion of GFP-GPI. Error bars represent SD; n > 10. Mean values for D were compared with an unpaired t test.

(C) Brefeldin A (BFA) treatment reduces total surface protein, as detected by labeling with membrane-impermeant, amine-reactive Cy5. FACS profiles for control and BFA-treated cells are shown; the fact that both populations of cells showed identical light-scattering properties indicates that BFA is unlikely to have significant effects on cell shape or size. Note that although Cy5 signal is plotted against intensity in the GFP channel, these cells were not transfected. p values are calculated with an unpaired t test.

(D) Lateral diffusion of LYFPGT46 construct in control and brefeldin-A-treated cells. Error bars represent SD; n = 10. Mean values for D were compared with an unpaired t test.

(E) Overexpression of CD9 is sufficient for increasing total surface protein, as detected by labeling with membrane-impermeant, amine-reactive Cy5. Cells transiently transfected with CD9-GFP was analyzed by FACS, and GFP fluorescence was plotted against Cy5 fluorescence. The numbered boxes show the brightest and faintest 30% of cells in the GFP channel; mean Cy5 fluorescence for these populations is shown in arbitrary units. p values are calculated with an unpaired t test.

(F) Lateral diffusion of LYFPGT46 construct in control (not transfected with CD9-CFP) and CD9-CFP overexpressing cells (highly overexpressing cells chosen by eye). Error bars represent SD; n = 10. Mean values for D were compared with an unpaired t test.

Increase or Reduction of Protein Density in Live Cells Causes Reciprocal Changes in Lateral Diffusion

The data presented above suggest that the actual density of proteins within the membrane is a significant factor in determining rates of lateral diffusion of membrane proteins. To confirm this more directly, we sought to alter the density of proteins within the PM of live cells. Cells were labeled with biotinylated ConA, and the bound ConA was patched with a combination of streptavidin and biotin antibodies (Figure 3A). We used a GPI-linked GFP construct as a probe for changes in lateral diffusion because this nonglycosylated construct was not itself concentrated in ConA patches. D for GPI-linked GFP is markedly decreased in regions of the PM containing capped ConA receptors (Figure 3B). This decrease in D confirms that patching and thereby increasing surface density of PM proteins is sufficient for local reduction of lateral diffusion.

In order to decrease total PM protein, we treated cells with Brefeldin A (BFA) and thereby prevented biosynthetic traffic to the PM. Changes in total protein content of the membrane were detected by labeling with membrane-impermeant, amine-reactive fluors (Cy3 or Cy5). Four hours of treatment with BFA decreased total surface protein by 16% (Figure 3C) and caused a concomitant 50% increase in D for LYFPGT46 (Figure 3D). To increase total protein, we overexpressed CD9-GFP by using optimized transfection conditions. This was sufficient for increasing total surface protein by 17% in the brightest 30% of CD9-GFP expressing cells (Figure 3E). FRAP of LYFPGT46 in the brightest CD9-CFP expressing cells revealed a 20% decrease in D (Figure 3F). These data provide direct evidence to show that even small changes to the total protein density in the membrane have a significant effect on the rate of lateral diffusion.

Our data show that for four proteins with different membrane topologies, the relatively slow diffusion over micron-scale distances observed in cells as opposed to artificial membrane systems is not dependent on interactions with cortical proteins and thus argue strongly against models where cortical barriers are a dominant factor in modulating micron-scale lateral diffusion in generic tissue-culture cell lines [1]. We propose an alternative model in which slow diffusion is an intrinsic property of the PM, and the density of proteins within the membrane has a significant effect on the observed

rates of diffusion. It is also possible that some specific proteins are effectively immobilized because of direct binding to cytoskeleton, but our data show that this can not provide a general explanation for slow diffusion in cell membranes. The FRAP experiments described here measure average rates of diffusion for populations of PM proteins and therefore do not provide information about the types of short-range translocation undergone by individual protein molecules. Thus, our data are not incompatible with the existence of anomalous diffusion because of effects of cortical barriers or other factors [1, 30]; rather, they argue that specifically cortical barriers do not have any large effect on overall rates of diffusion over micron-scale distances [17–19].

Experimental Procedures

FRAP and data analyses were carried out as described [9]. Ventral membrane sheets were prepared according to the method of Cattelino et al. [26]. Detailed Experimental Procedures are available online.

Supplemental Data

Supplemental Data include Experimental Procedures, six figures, and one movie and are available with this article online at http://www.current-biology.com/cgi/content/full/17/5/462/DC1/.

Acknowledgments

R. Grenfell gave expert assistance with FACS experiments. All those who provided plasmids are thanked.

Received: October 3, 2006
Revised: January 4, 2007
Accepted: January 22, 2007
Published online: March 1, 2007

References

1. Kusumi, A.A., Nakada, C., Ritchie, K., Murase, K., Suzuki, K., Murakoshi, H., Kasai, R.S., Kondo, J., and Fujiwara, T. (2005). Paradigm shift of the plasma membrane concept from the two-dimensional continuum fluid to the partitioned fluid: High-speed single-molecule tracking of membrane molecules. Annu. Rev. Biophys. Biomol. Struct. *34*, 351–378.
2. Saxton, M.J., and Jacobson, K. (1997). Single-particle tracking: Applications to membrane dynamics. Annu. Rev. Biophys. Biomol. Struct. *26*, 373–399.
3. Kucik, D.F., Elson, E.L., and Sheetz, M.P. (1999). Weak dependence of mobility of membrane protein aggregates on aggregate size supports a viscous model of retardation of diffusion. Biophys. J. *76*, 314–322.
4. Ryan, T.A., Myers, J., Holowka, D., Baird, B., and Webb, W.W. (1988). Molecular crowding on the cell surface. Science *239*, 61–64.
5. Axelrod, D., Koppel, D.E., Schlessinger, J., Elson, E., and Webb, W.W. (1976). Mobility measurement by analysis of fluorescence photobleaching recovery kinetics. Biophys. J. *16*, 1055–1069.
6. Feder, T.J., Brust-Mascher, I., Slattery, J.P., Baird, B., and Webb, W.W. (1996). Constrained diffusion or immobile fraction on cell surfaces: A new interpretation. Biophys. J. *70*, 2767–2773.
7. Sbalzarini, I.F., Hayer, A., Helenius, A., and Koumoutsakos, P. (2006). Simulations of (an)isotropic diffusion on curved biological surfaces. Biophys. J. *90*, 878–885.
8. Braga, J., Desterro, J.M., and Carmo-Fonseca, M. (2004). Intracellular macromolecular mobility measured by fluorescence recovery after photobleaching with confocal laser scanning microscopes. Mol. Biol. Cell *15*, 4749–4760.
9. Schmidt, K., and Nichols, B.J. (2004). A barrier to lateral diffusion in the cleavage furrow of dividing mammalian cells. Curr. Biol. *14*, 1002–1006.
10. Kenworthy, A.K., Nichols, B.J., Remmert, C.L., Hendrix, G.M., Kumar, M., Zimmerberg, J., and Lippincott-Schwartz, J. (2004). Dynamics of putative raft-associated proteins at the cell surface. J. Cell Biol. *165*, 735–746.
11. Chen, Y., Lagerholm, B.C., Yang, B., and Jacobson, K. (2006). Methods to measure the lateral diffusion of membrane lipids and proteins. Methods *39*, 147–153.
12. Lippincott-Schwartz, J., Snapp, E., and Kenworthy, A. (2001). Studying protein dynamics in living cells. Nat. Rev. Mol. Cell Biol. *2*, 444–456.
13. Toomre, D., Steyer, J.A., Keller, P., Almers, W., and Simons, K. (2000). Fusion of constitutive membrane traffic with the cell surface observed by evanescent wave microscopy. J. Cell Biol. *149*, 33–40.
14. Poo, M. (1982). Rapid lateral diffusion of functional A Ch receptors in embryonic muscle cell membrane. Nature *295*, 332–334.
15. Tank, D.W., Wu, E.S., and Webb, W.W. (1982). Enhanced molecular diffusibility in muscle membrane blebs: Release of lateral constraints. J. Cell Biol. *92*, 207–212.
16. Kahya, N., Brown, D.A., and Schwille, P. (2005). Raft partitioning and dynamic behavior of human placental alkaline phosphatase in giant unilamellar vesicles. Biochemistry *44*, 7479–7489.
17. Vrljic, M., Nishimura, S.Y., Brasselet, S., Moerner, W.E., and McConnell, H.M. (2002). Translational diffusion of individual class II MHC membrane proteins in cells. Biophys. J. *83*, 2681–2692.
18. Nishimura, S.Y., Vrljic, M., Klein, L.O., McConnell, H.M., and Moerner, W.E. (2006). Cholesterol depletion induces solid-like regions in the plasma membrane. Biophys. J. *90*, 927–938.
19. Fujiwara, T., Ritchie, K., Murakoshi, H., Jacobson, K., and Kusumi, A. (2002). Phospholipids undergo hop diffusion in compartmentalized cell membrane. J. Cell Biol. *157*, 1071–1081.
20. Schmidt, K., and Nichols, B.J. (2004). Functional interdependence between septin and actin cytoskeleton. BMC Cell Biol. *5*, 43.
21. Kinoshita, M., Field, C.M., Coughlin, M.L., Straight, A.F., and Mitchison, T.J. (2002). Self- and actin-templated assembly of mammalian septins. Dev. Cell *3*, 791–802.
22. Cooper, J.A., Bryan, J., Schwab, B., 3rd, Frieden, C., Loftus, D.J., and Elson, E.L. (1987). Microinjection of gelsolin into living cells. J. Cell Biol. *104*, 491–501.
23. Cunningham, C.C., Gorlin, J.B., Kwiatkowski, D.J., Hartwig, J.H., Janmey, P.A., Byers, H.R., and Stossel, T.P. (1992). Actin-binding protein requirement for cortical stability and efficient locomotion. Science *255*, 325–327.
24. Sheetz, M.P., Schindler, M., and Koppel, D.E. (1980). Lateral mobility of integral membrane proteins is increased in spherocytic erythrocytes. Nature *285*, 510–511.
25. Tomishige, M., Sako, Y., and Kusumi, A. (1998). Regulation mechanism of the lateral diffusion of band 3 in erythrocyte membranes by the membrane skeleton. J. Cell Biol. *142*, 989–1000.
26. Cattelino, A., Albertinazzi, C., Bossi, M., Critchley, D.R., and de Curtis, I. (1999). A cell-free system to study regulation of focal adhesions and of the connected actin cytoskeleton. Mol. Biol. Cell *10*, 373–391.
27. Way, M., Pope, B., and Weeds, A.G. (1992). Evidence for functional homology in the F-actin binding domains of gelsolin and alpha-actinin: Implications for the requirements of severing and capping. J. Cell Biol. *119*, 835–842.
28. Jacobson, K., Sheets, E.D., and Simson, R. (1995). Revisiting the fluid mosaic model of membranes. Science *268*, 1441–1442.
29. Glebov, O.O., and Nichols, B.J. (2004). Lipid raft proteins have a random distribution during localized activation of the T-cell receptor. Nat. Cell Biol. *6*, 238–243.
30. Lenne, P.F., Wawrezinieck, L., Conchonaud, F., Wurtz, O., Boned, A., Guo, X.J., Rigneault, H., He, H.T., and Marguet, D. (2006). Dynamic molecular confinement in the plasma membrane by microdomains and the cytoskeleton meshwork. EMBO J. *25*, 3245–3256.
31. Keller, P., Toomre, D., Diaz, E., White, J., and Simons, K. (2001). Multicolour imaging of post-Golgi sorting and trafficking in live cells. Nat. Cell Biol. *3*, 140–149.